

Synchronization Strategy Research of Pneumatic Servo System Based on Separate Control of Meter-in and Meter-out

Xiaocong Zhu, Jian Cao, Guoliang Tao, Bin Yao *Member, IEEE*

Abstract—In the pneumatic synchronization system based on separate control of meter-in and meter-out, both motion trajectory and pressure trajectory could be tracked in a single pneumatic cylinder and then the cylinder could be controlled completely without internal dynamics. In this paper, an adaptive robust pressure controller is used to keep the pressure level in chamber of cylinder on an even keel when the pneumatic cylinder is moving, which will result in small variation of cylinder's friction force and facilitate the precise modeling of friction force, and an adaptive robust motion controller is designed to improve the motion tracking accuracy of pneumatic cylinder, and on-line parameter estimation of the flow coefficient is utilized to have improved model compensation, and moreover a synchronization controller is added to further reduce the synchronization error. Experimental results demonstrate that this synchronization strategy could not only make two cylinders synchronized moving accurately, but also obtain very smooth control inputs which indicate the effectiveness of model compensation.

I. INTRODUCTION

The compressibility of air and the inherent nonlinearity of pneumatic systems continue to make achieving accurate position tracking control a challenging problem [1]. Though pneumatic position servo control has been researched for over twenty years and servo-pneumatic positioning systems of FESTO Company have been widely used in industrial applications to realize stepless position control from point to point, the research on pneumatic synchronization control is rising up recently and can be divided into two stages. In the first stage, position trajectory tracking of one cylinder develops to position trajectory tracking of several cylinders and synchronization errors between several cylinders are not used for feedback control. For example, Pandian *et al* proposed a new sliding mode controller using differential pressure to avoid the need for acceleration feedback, and successfully applied this controller to the synchronized motion of two vertical cylinders[2]. Maeda *et al* realized the precise position control of a pneumatic lifter by using a dither to decrease nonlinear characteristics of friction and a disturbance observer to increase robustness [3]. Zhao designed two controllers for an electro-pneumatic synchro system, the one is an inner-outer loop feedback synchro con-

troller combined with input-output linearization and friction compensation, and the other is a two-folded sliding mode synchro controller with friction compensation [4]. In the second stage, the synchronization error would be feed to a synchronization controller and the output of which will be added to respective motion controllers. For example, Jang *et al* proposed a synchronization position controller with a position controller to reduce effects of nonlinear characteristics and a synchronization controller to reduce synchronization error [5]. For the synchronization control of two vertical-type pneumatic servo systems, Shibata *et al* adopted a fuzzy controller in each cylinder so that the output of each plant can follow the reference input and simultaneously a PD controller to realize the synchronization motion of two cylinders [6].

In the traditional pneumatic position servo system controlled by one proportional directional valve, meter-in and meter-out orifices are mechanically linked, which results in large air consumption, easily saturated control input and small amplitude vibrations due to internal dynamics [7]. Therefore, the pneumatic system based on separate control of meter-in and meter-out would be adopted to realize high precision synchronization motion. Generally, the pneumatic system based on separate control has three types of structural components. Firstly, two proportional directional valves control one cylinder [3], [5], [7], [8]. This type has the advantage of fast response and disadvantages of requiring the technique of computational flow feedback and bringing about the complexity of controller due to more than three orders of system model. Secondly, two proportional pressure valves control one cylinder [6], [9]. This type needn't consider the regulating process of pressure and then reduce the order of system model. But, the proportional pressure valve has large time delay due to the compressibility of air. If two proportional pressure valves are fed by varying control inputs simultaneously, the control performance would be worse. So, the control input of one pressure valve would be constant in practical. Thirdly, several fast switching valves control one cylinder [10]. This type has advantages of cheapness and strong anti-interference due to PWM control. Meanwhile, disadvantages of this type are deadzone and nonlinearity at original point of differential pressure-duty cycle curve.

The high-precision position control of a parallel manipulator driven by pneumatic muscles is realized through applying adaptive robust control(ARC) strategy to it [11]. Thus, it is an attempt that applying this strategy to the rodless pneumatic cylinder with large friction force for achieving the high-precision synchronization motion. The adaptive robust

This work is supported by National Natural Science Foundation of China (No. 50775200).

Xiaocong Zhu, Jian Cao and Guoliang Tao are with the State Key Laboratory of Fluid Power Transmission and Control, Zhejiang University, Hangzhou 310027, China zhuxiaoc@zju.edu.cn, caojianjiaowang@sina.com, gltao@zju.edu.cn. Bin Yao is with The State Key Laboratory of Fluid Power Transmission and Control, Zhejiang University, Hangzhou 310027, China and also with Purdue University, West Lafayette, IN 47907-2040, USA byao@purdue.edu.

pressure controller designed in reference [12] has two merits in this paper. Firstly, the adaptive robust pressure controller can keep the pressure level in chamber of cylinder on an even keel when the pneumatic cylinder is moving, which will result in small variation of cylinder's friction force and facilitate the precise modeling of friction force. Secondly, in the adaptive robust motion controller based on backstepping design, the first layer is the pressure control. Therefore, only if the pressure control tends to asymptotically stable and achieve high precision, so will be the motion control. On the basis of the research on pressure trajectory tracking of ARC [12], an adaptive robust motion controller is designed to improve the motion tracking accuracy of pneumatic cylinder, and on-line parameter estimation of the flow coefficient is utilized to have improved model compensation, and moreover a synchronization controller is added to further reduce the synchronization error.

II. SYSTEM DYNAMICS

A. Synchronous Schematic Diagram of Pneumatic Servo System

The synchronous schematic diagram of pneumatic servo system is shown in Fig. 1. Two proportional directional valves(MPYE-5-1/8-HF-010B by FESTO) separately control two chambers of a rodless pneumatic cylinder(DGPIL-25-500-6K-KF-AU by FESTO), and pressure transducers(SDET-22T-D10-G14-I-M12 by FESTO) are used to measure pressures of chamber A, chamber B and supply pressure respectively, and position transducers(RPS0500MD601 V810050 by MTS) are used to measure positions and velocities of two rodless pneumatic cylinders. Since two valves separately control two chambers of a cylinder, there exist two control degrees of freedom, thus two different trajectories can be controlled, for example, motion trajectory and pressure trajectory, motion trajectory and energy trajectory, or motion trajectory and stiffness trajectory. Moreover, a cylinder could be controlled completely since there is no internal dynamics. In this paper, chamber A is regulated by an adaptive robust motion controller to track a motion trajectory while chamber B is regulated by an adaptive robust pressure controller to track a pressure trajectory and the output of synchronization controller is added to respective adaptive robust motion controllers for further reducing the synchronization error.

B. Motion Dynamics of Pneumatic Cylinder

The motion dynamics of the rodless cylinder is

$$M\ddot{x} = (p_a A_a - p_b A_b) + (A_b - A_a)p_{atm} - F_f - F_w + d_F(t) \quad (1)$$

where x is the position of piston, M is the mass including piston, slider and external loads, p_a and A_a is the absolute pressure and acting area of chamber A respectively, p_b and A_b is the absolute pressure and acting area of chamber B respectively, p_{atm} is the local atmospheric pressure, F_f is the friction force, F_w is the external force, $d_F(t)$ is the lumped disturbance including pressure error, mass error, friction force error and external force error. When the counter

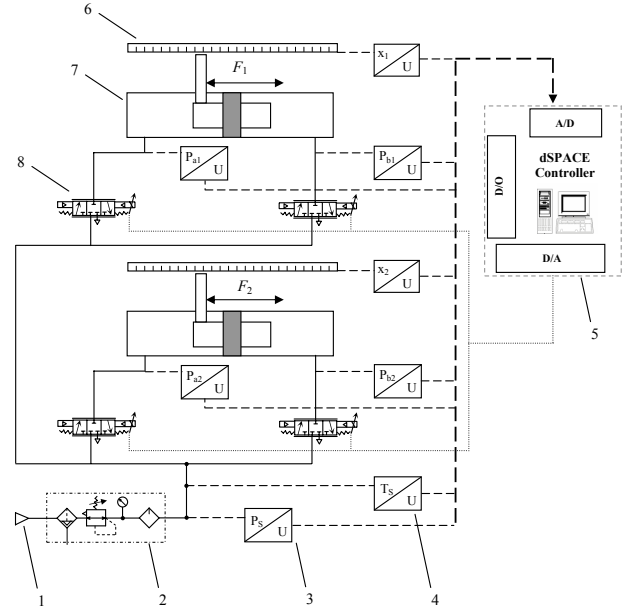


Fig. 1. Synchronous schematic diagram of pneumatic servo system
1.air supply 2.air treatment unit 3.pressure transducer 4.temperature transducer 5.dSPACE controller 6.position transducer 7.rodless pneumatic cylinder 8.proportional directional valve

pressure p_b is approximately constant, the friction force is described by

$$F_f = \left[F_d + (F_s - F_d) e^{-(\dot{x}/\dot{x}_s)} \right] \tanh\left(\frac{\dot{x}}{\eta}\right) + f_v \dot{x} \quad (2)$$

where F_d is the Coulumb dynamic friction, F_s is the maximum static friction, \dot{x}_s is the Stribeck velocity, f_v is the viscous friction coefficient, η is a positive parameter.

C. Pressure Dynamics in Pneumatic Cylinder

According to state equation of ideal gas, continuity equation for steady one-dimensional flow, and the first law of thermodynamics [13], an integrated expression of pressure dynamics is presented by Richer and Hurmuzlu as following Eq.(3) and Eq.(4) in which $\alpha_{in} = 1.4$, $\alpha_{out} = 1.0$, $\alpha = 1.2$.

$$\dot{p}_a = \frac{RT_s}{V_a} (\alpha_{in} q_{ain} - \alpha_{out} q_{aout}) - \alpha \frac{p_a A_a}{V_a} \dot{x} + d_{pa}(t) \quad (3)$$

$$\dot{p}_b = \frac{RT_s}{V_b} (\alpha_{in} q_{bin} - \alpha_{out} q_{bout}) + \alpha \frac{p_b A_b}{V_b} \dot{x} + d_{pb}(t) \quad (4)$$

where R is the ideal gas constant, T_s is the upstream temperature of proportional directional valve, V_a and V_b are volumes in chamber A and chamber B respectively, q_{ain} and q_{aout} are mass flow rates flowing in and out of chamber A respectively, q_{bin} and q_{bout} are mass flow rates flowing in and out of chamber B respectively, $d_{pa}(t)$, $d_{pb}(t)$ are lumped disturbances of pressure dynamics, which include modeling errors of pressure dynamics and mass flow rate through orifice and temperature variation.

D. Mass Flow Rate of Proportional Directional Valve

The critical pressure ratio p_{cr} obtained from the Bernoulli's law and isentropic process is significantly different from the critical pressure ratio b obtained from ISO6358. For guaranteeing the effectiveness of model compensation, the experimental value of critical pressure ratio b would be used to localize the boundary between sonic and subsonic flows. At the same time, for keeping the segment function continuous, the following equation of mass flow rate will be adopted [14].

$$q = A_e C_q C_m \frac{p_s}{\sqrt{T_s}} \quad (5)$$

where A_e is the orifice area, C_q is the flow coefficient, p_s is the supply pressure and the flow parameter C_m is given by

$$C_m = \begin{cases} \sqrt{\frac{\gamma}{R} \left(\frac{2}{\gamma+1} \right)^{\frac{\gamma+1}{\gamma-1}}} & 0 < \frac{p_b}{p_s} \leq b \\ C_t \sqrt{\frac{2\gamma}{R(\gamma-1)}} \sqrt{1 - \left(\frac{\frac{p_b}{p_s} - b}{1-b} \right)^2} & b < \frac{p_b}{p_s} \leq \lambda \\ \frac{\left(\frac{p_b}{p_s} \right) - 1}{\lambda - 1} C_t \sqrt{\frac{2\gamma}{R(\gamma-1)}} \sqrt{1 - \left(\frac{\lambda - b}{1-b} \right)^2} & \lambda < \frac{p_b}{p_s} \end{cases} \quad (6)$$

in which λ is the minimal pressure ratio to have a laminar flow, C_t is a correction factor between theoretical and experimental critical pressure ratios.

III. CONTROLLER DESIGN

There exist nonlinearities of motion dynamics, pressure dynamics and mass flow rate, and moreover many parameters and external disturbances are unknown. So, it is necessary to apply adaptive robust control strategy on the basis of the explicit nonlinear models to the pneumatic servo system based on separate control of meter-in and meter-out for achieving the synchronization motion.

A. Adaptive Robust Pressure Controller

The adaptive robust pressure controller is used to keep the pressure level in chamber B on an even keel when pneumatic cylinders are moving. As the length of paper is limited, the detailed design procedure of the adaptive robust pressure controller can refer to [12].

B. Adaptive Robust Motion Controller

Generally, the lumped disturbance $d_F(t)$ in motion dynamics may be decomposed into two parts, the constant or slow time-varying part denoted by d_{F0} and the fast time-varying part denoted by $\tilde{d}_F(t)$, i.e., $d_F(t) = d_{F0} + \tilde{d}_F(t)$. Similarly, $d_p(t)$ in pressure dynamics could also be decomposed into two parts, i.e., $d_{pa}(t) = d_{pa0} + \tilde{d}_{pa}(t)$. Furthermore, unknown parameters C_q in Eq.5, d_{F0} in Eq.1 and d_{pa0} in Eq.3 are updated by on-line parameter estimation to improve control accuracy, and meanwhile, a discontinuous projection mapping is utilized to guarantee that parameter estimates and their derivatives remain in the known bounded regions all the time [15]. Then the adaptive robust motion controller based on backstepping design is synthesized as follows.

1) Step 1

Let z_1 be the motion tracking error.

$$z_1 = x - x_d \quad (7)$$

where x_d is the desired motion trajectory.

Define a switching-function-like quantity as

$$z_2 = \dot{z}_1 + k_1 z_1 = \dot{x} - \dot{x}_d + k_1 z_1 \quad (8)$$

where k_1 is a positive parameter.

Let $\dot{x}_r = \dot{x}_d - k_1 z_1$ and Eq.8 is rewritten as

$$z_2 = \dot{x} - \dot{x}_r \quad (9)$$

where \dot{x}_r can be regarded as a corrected desired motion velocity and then z_2 is regarded as a kind of velocity error in a certain degree.

Differentiate Eq.9 and substitute Eq.1 into it, one obtains

$$\dot{z}_2 = \frac{A_a}{M} p_a + \frac{1}{M} [-p_b A_b + (A_b - A_a) p_{atm} - F_f - F_w - M \ddot{x}_r + d_{F0} + \tilde{d}_F(t)] \quad (10)$$

Consider p_a in Eq.10 as the virtual control input. Next is to design the desired virtual pressure p_{ad} for making the output tracking error z_2 converge to zero or a small value with a guaranteed transient performance.

The desired virtual pressure p_{ad} can be defined as

$$p_{ad} = p_{ada} + p_{ads} \quad (11)$$

$$p_{ada} = \frac{1}{A_a} [p_{bd} A_b + (A_a - A_b) p_{atm} + F_f + F_w + M \ddot{x}_r - \hat{d}_{F0}] \quad (12)$$

where p_{ada} is a model compensation term and p_{ads} is a robust feedback term, which consists of the following two parts.

$$p_{ads} = p_{ads1} + p_{ads2} \quad (13)$$

$$p_{ads1} = -\frac{M}{A_a} k_2 z_2 \quad (14)$$

where k_2 is a positive parameter and p_{ads2} is chosen to satisfy the following conditions.

$$\begin{cases} z_2 \frac{1}{M} (A_a p_{ads2} - \tilde{d}_{F0} + \tilde{d}_F(t)) < \varepsilon_2 \\ z_2 \frac{1}{M} A_a p_{ads2} < 0 \end{cases} \quad (15)$$

where ε_2 is a positive design parameter.

Denote the virtual control input discrepancy as $z_3 = p_a - p_{ad}$. Substituting Eq.11 ~ Eq.15 into Eq.10, one obtains

$$\dot{z}_2 = -k_2 z_2 + \frac{1}{M} (A_a p_{ads2} - \tilde{d}_{F0} + \tilde{d}_F(t)) + \frac{A_a}{M} z_3 \quad (16)$$

Define a positive semi-definite Lyapunov function as $V_2 = \frac{1}{2} z_2^2$, the time derivative of V_2 is

$$\dot{V}_2 = -k_2 z_2^2 + z_2 \frac{1}{M} (A_a p_{ads2} - \tilde{d}_{F0} + \tilde{d}_F(t)) + \frac{A_a}{M} z_2 z_3 \quad (17)$$

Assume z_3 converges to zero in the process of controlling, substitute the first equation of Eq.15 into Eq.17, and then obtain

$$\dot{V}_2 \leq -k_2 z_2^2 + \varepsilon_2 \quad (18)$$

To determine the adaptation law, define another Lyapunov function as $V_{2a} = V_2 + \frac{1}{2}\Gamma_2^{-1}\tilde{d}_{F0}^2$ and its time derivative is

$$\begin{aligned}\dot{V}_{2a} &= -k_2z_2^2 + z_2\frac{1}{M}(A_a p_{ads2} - \tilde{d}_{F0} + \tilde{d}_F(t)) + \frac{A_a}{M}z_2z_3 \\ &\quad + \Gamma_2^{-1}\tilde{d}_{F0}\dot{\tilde{d}}_{F0} \\ &= -k_2z_2^2 + \frac{z_2}{M}(A_a p_{ads2} + \tilde{d}_F(t)) + \frac{A_a}{M}z_2z_3 + \Gamma_2^{-1}\tilde{d}_{F0}\dot{\tilde{d}}_{F0} \\ &\quad - \frac{z_2}{M}\tilde{d}_{F0}\end{aligned}\quad (19)$$

The adaptation function is given by

$$\dot{\tilde{d}}_{F0} = \text{Proj}_{\tilde{d}_{F0}}\left(\Gamma_2\frac{z_2}{M}\right) \quad (20)$$

Substitute Eq.20 into Eq.19 while noting $\dot{\tilde{d}}_{F0} = \dot{\tilde{d}}_{F0}$, one obtains

$$\dot{V}_{2a} = -k_2z_2^2 + \frac{z_2}{M}(A_a p_{ads2} + \tilde{d}_F(t)) + \frac{A_a}{M}z_2z_3 \quad (21)$$

2) Step 2

Define the virtual mass flow rate as $q_m = \alpha_{in}q_{ain} - \alpha_{out}q_{aout}$, the next step is to synthesize the desired virtual mass flow rate q_{md} so that z_3 converges to zero or a small value with a guaranteed transient performance.

According to Eq.3, the time derivative of z_3 is given by

$$\dot{z}_3 = \dot{p}_a - \dot{p}_{ad} = \frac{RT_s}{V_a}q_{ma} - \alpha\frac{p_a A_a}{V_a}\dot{x} + d_{pa0} - \dot{p}_{adc} - \dot{p}_{adu} + \tilde{d}_{pa}(t) \quad (22)$$

where $\dot{p}_{adc} = \frac{\partial P_{ad}}{\partial x}\dot{x} + \frac{\partial P_{ad}}{\partial \hat{x}}\hat{\dot{x}} + \frac{\partial P_{ad}}{\partial t}$,

$\dot{p}_{adu} = \frac{\partial P_{ad}}{\partial \hat{d}_{F0}}\dot{\hat{d}}_{F0} + \frac{\partial P_{ad}}{\partial \hat{x}}(\ddot{x} - \hat{\ddot{x}})$, in which \dot{p}_{adc} represents the calculable part of \dot{p}_{ad} , and $\hat{\ddot{x}}$ is the estimated acceleration, which is deduced from \dot{x} through a differential filter, \dot{p}_{adu} represents the incalculable part of \dot{p}_{ad} . The influence of \dot{p}_{adu} is included in the lumped disturbance $d_{pa}(t)$ and can be attenuated by robust feedback term.

The desired virtual mass flow rate is

$$q_{md} = q_{mda} + q_{mds} \quad (23)$$

$$q_{mda} = \alpha\frac{p_a A_a}{RT_s}\dot{x} - \frac{V_a}{RT_s}\hat{d}_{pa0} + \frac{V_a}{RT_s}\dot{p}_{adc} - \frac{V_a A_a}{RT_s M}z_2 \quad (24)$$

where q_{mda} is a model compensation term in which \hat{d}_{pa0} is updated by on-line parameter adaptation and q_{mds} is a robust feedback term, which consists of the following two parts.

$$q_{mds} = q_{mds1} + q_{mds2} \quad (25)$$

$$q_{mds1} = -k_3z_3\frac{V_a}{RT_s} \quad (26)$$

q_{mds2} is synthesized to dominate the uncompensated model uncertainties coming from both parametric uncertainties and uncertain nonlinearities, which is chosen to satisfy the following conditions.

$$\begin{cases} z_3\left(\frac{RT_s}{V_a}q_{mds2} - \tilde{d}_{pa0} + \tilde{d}_{pa}(t) - \dot{p}_{adu}\right) \leq \varepsilon_3 \\ z_3\frac{RT_s}{V_a}q_{mds2} \leq 0 \end{cases} \quad (27)$$

where ε_3 is a positive design parameter.

Define a positive semi-definite Lyapunov function as $V_3 = V_2 + \frac{1}{2}z_3^2$, the time derivative of V_3 is

$$\begin{aligned}\dot{V}_3 &= -k_2z_2^2 - k_3z_3^2 + z_2\frac{1}{M}(A_a p_{ads2} - \tilde{d}_{F0} + \tilde{d}_F(t)) \\ &\quad + z_3\left(\frac{RT_s}{V_a}q_{mds2} - \tilde{d}_{pa0} + \tilde{d}_{pa}(t) - \dot{p}_{adu}\right)\end{aligned} \quad (28)$$

Substitute the first equations of Eq.15 and Eq.27 into Eq.28, one obtains

$$\dot{V}_3 \leq -k_3z_3^2 - k_2z_2^2 + \varepsilon_3 + \varepsilon_2 \quad (29)$$

Thus, z_2 and z_3 will exponentially converge to some balls whose sizes are proportional to ε_2 and ε_3 , and then be ultimately bounded.

To determine the adaptation law, define another Lyapunov function as $V_{3a} = V_3 + \frac{1}{2}\Gamma_3^{-1}\tilde{d}_{pa0}^2$. According to Eq.28, the time derivative of V_{3a} is

$$\begin{aligned}\dot{V}_{3a} &= -k_2z_2^2 + \frac{z_2}{M}(A_a p_{ads2} + \tilde{d}_F(t)) + \Gamma_2^{-1}\tilde{d}_{F0}\dot{\tilde{d}}_{F0} - \frac{z_2}{M}\tilde{d}_{F0} \\ &\quad - k_3z_3^2 + z_3\left(\frac{RT_s}{V_a}q_{mds2} + \tilde{d}_{pa}(t)\right) + \Gamma_3^{-1}\tilde{d}_{pa0}\dot{\tilde{d}}_{pa0} - z_3\tilde{d}_{pa0}\end{aligned} \quad (30)$$

The adaptation function is given by

$$\dot{\tilde{d}}_{pa0} = \text{Proj}_{\tilde{d}_{pa0}}(\Gamma_3z_3) \quad (31)$$

Substitute Eq.20 and Eq.31 into Eq.30 while noting $\dot{\tilde{d}}_{F0} = \dot{\tilde{d}}_{F0}$ and $\dot{\tilde{d}}_{pa0} = \dot{\tilde{d}}_{pa0}$, one obtains

$$\begin{aligned}\dot{V}_{3a} &= -k_2z_2^2 - k_3z_3^2 + \frac{z_2}{M}(A_a p_{ads2} + \tilde{d}_F(t)) \\ &\quad + z_3\left(\frac{RT_s}{V_a}q_{mds2} + \tilde{d}_{pa}(t)\right)\end{aligned} \quad (32)$$

If the system is devoid of uncertain nonlinearities, (i.e., $\tilde{d}_F(t) = 0, \tilde{d}_{pa}(t) = 0$). According to the second equations of Eq.15 and Eq.27, one obtains

$$\dot{V}_{3a} \leq -k_2z_2^2 - k_3z_3^2 \quad (33)$$

Hence, asymptotic output tracking (or zero final tracking error) is obtained as well.

3) Step 3

C_q is also updated by on-line parameter estimation according to the pressure dynamics Eq.3 for further reducing model errors. To bypass the problem that numerical differentiation of pressure feedback signal would result in severe noise if it were adopted by parameter estimation, a stable filter with a relative degree larger than or equal to 1 would be employed in the pressure dynamics and $\tilde{d}_{pa}(t) = 0$ would be assumed [16], and then a standard linear regression model for parameter estimation could be obtained.

$$y = \dot{p}_{af} = \Phi_{4f}^T \beta + y_n \quad (34)$$

where \dot{p}_{af} is the filtered output of \dot{p}_a , Φ_{4f} is the corresponding regressor of unknown parameter β and $\beta = C_q$.

The least squares type estimation algorithm is used to estimate the unknown parameter β [16], and a discontinuous

projection mapping is used to keep parameter estimates bounded. β is updated by an adaptation law as

$$\dot{\hat{\beta}} = \text{Proj}_{\hat{\beta}} (\Gamma_4 \sigma_4) \quad (35)$$

with the adaptation function given by

$$\sigma_4 = -\frac{1}{1 + v \cdot \text{tr}\{\varphi_{4f}^T \Gamma_4 \varphi_{4f}\}} \varphi_{4f} \Gamma_4 \quad (36)$$

and the adaptation rate matrix given by

$$\dot{\Gamma}_4 = \alpha_4 \Gamma_4 - \frac{1}{1 + v \cdot \text{tr}\{\varphi_{4f}^T \varphi_{4f}\}} \Gamma_4 \varphi_{4f} \varphi_{4f}^T \Gamma_4 \quad (37)$$

where $\alpha_4 \geq 0$ is the forgetting factor, and $v \geq 0$.

4) Step 4

After q_{md} and C_q is calculated, the control input of proportional directional valve could be obtained according to the equation of mass flow rate (Eq.5) and the relation between control voltage and orifice area [12].

C. Synchronization Controller

Considering that two pneumatic cylinders may have different characteristics and suffer from different working environments, a PID-type synchronization controller is designed and its output is added to two respective adaptive robust motion controllers for further reducing the synchronization error.

The synchronization error between two cylinders is

$$e_s = e_{x1} - e_{x2} \quad (38)$$

where e_{x1} and e_{x2} are position tracking errors of cylinder 1 and cylinder 2 respectively.

The output of the synchronous controller is

$$u_s(k+1) = k_p e_s(k) + k_i \sum_{i=0}^{k-1} e_s(k-i) + k_d \frac{e_s(k) - e_s(k-1)}{T} \quad (39)$$

where k_p , k_i and k_d are proportional gain, integral gain and derivative gain respectively and T is sampling period.

The control inputs of two adaptive robust motion controllers are respectively corrected.

$$u_{2c} = u_2 - u_s \quad (40)$$

$$u_{3c} = u_3 + u_s \quad (41)$$

Thus, the synchronization motion of two pneumatic cylinders can be realized on the basis of each cylinder tracking the same desired position trajectory even in the presence of large disturbances and modeling errors.

D. Synchronization Principle

Putting all the procedures together, the synchronization principle of pneumatic servo system is schematically presented in Fig.2.

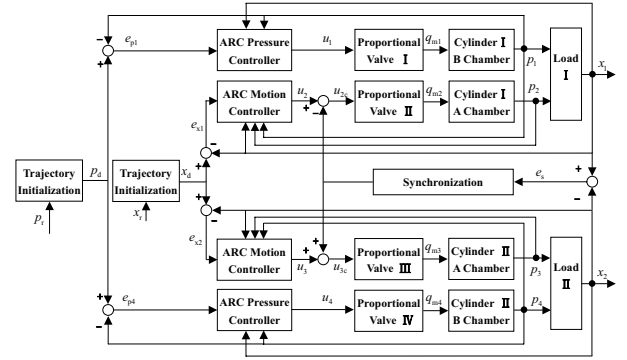


Fig. 2. Synchronization motion principle of pneumatic servo system

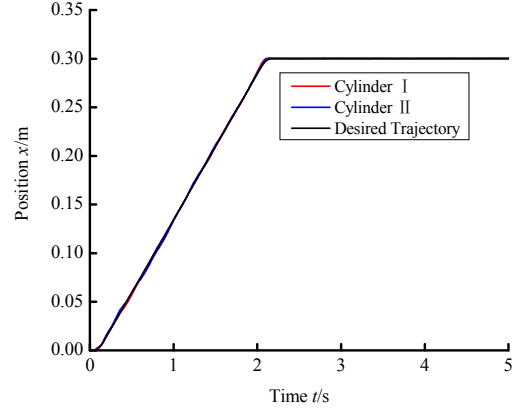


Fig. 3. Position tracking responses of two cylinders

IV. EXPERIMENTAL RESULTS

The effectiveness of the proposed controllers is demonstrated by the actual synchronization motion of two pneumatic cylinders tracking a step trajectory through trajectory initialization. In the experiment, the supply pressure is 0.5MPa, the desired counter pressure is 0.2MPa and the expected position is 0.3m. Fig.3 shows position tracking responses of two rodless pneumatic cylinders. Fig.4 is tracking errors and synchronization error of two cylinders. Fig.5 shows pressure responses inside four chambers of two cylinders. As can be seen from Fig.3 and Fig.4, tracking errors of each pneumatic cylinder and the synchronization error of two cylinders are very small with maximum tracking errors less than 0.0032m and maximum synchronization error less than 0.0033m. It can be seen from Fig.5 that there is large pressure discrepancy between chambers A of two cylinders and little pressure discrepancy between chambers B when pneumatic cylinders are moving. This illustrates that friction forces of two cylinders are quite different. Fortunately, parameter estimation of lumped disturbance and flow rate coefficient in the proposed controllers could compensate such model errors and then small position tracking errors are realized in rodless pneumatic cylinders with large friction force. It can also be seen from Fig.6, control inputs of two proportional directional valves for motion controlling are all very smooth, which verified the effectiveness of model compensation.

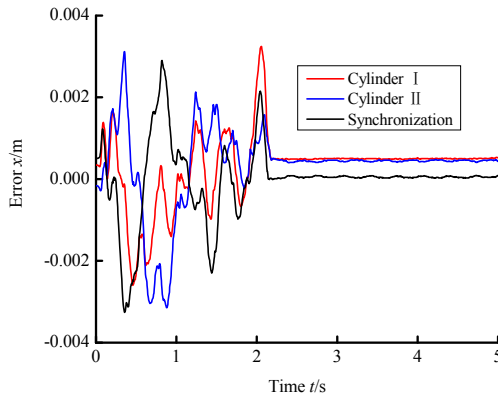


Fig. 4. Tracking errors and synchronization error of two cylinders

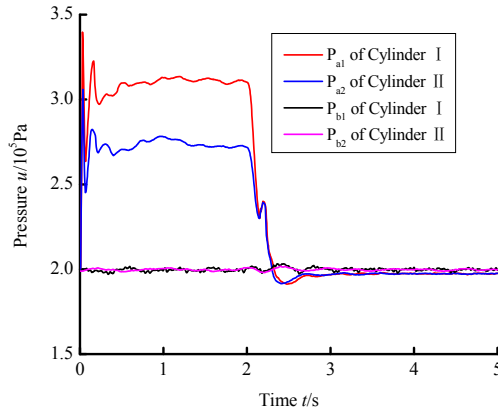


Fig. 5. Pressure responses inside four chambers of two cylinders

V. CONCLUSIONS

For the pneumatic servo system based on separate control of meter-in and meter-out, adaptive robust control strategy is applied to the rodless pneumatic cylinder with large friction force for achieving the synchronization motion. Thereinto, an adaptive robust pressure controller is used to keep the pressure level in chamber B of each cylinder on an even keel when pneumatic cylinders are moving, which will result in small variation of cylinder's friction force and facilitate the precise modeling of friction force, and an adaptive robust motion controller is designed to control chamber A and improve the motion tracking accuracy, on-line parameter estimation of the flow coefficient is utilized to have improved model compensation, and moreover the synchronization error would be fed to a synchronization controller in order to further reduce the synchronization error. For tracking a initialized step position trajectory, maximum synchronization error is less than 0.0033m with smooth control inputs, which verifies the effectiveness of the synchronization control strategy and model compensation.

REFERENCES

[1] S. Ning and G. M. Bone, Experimental comparison of position tracking control algorithms for pneumatic cylinder actuators, *IEEE/ASME Transactions on Mechatronics*, vol.12,no.5,2007, pp 557-561.

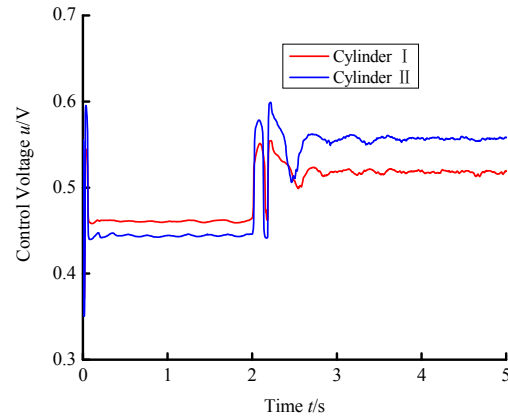


Fig. 6. Control inputs of two proportional directional valves for motion controlling

[2] S. R. Pandian, Y. Hayakawa, Y. Kanazawa *et al*, Practical design of a sliding mode controller for pneumatic actuators, *Transactions of the ASME, Journal of Dynamic systems, Measurement and Control*, vol.119, no.4, 1997, pp 666-674.

[3] S. Maeda, Y. Kawakami and K. Nakano, Position control of pneumatic lifters, *Transactions of the Japan Hydraulics & Pneumatics Society*, vol.30, no.4, 1999, pp 89-95.

[4] Zhao Hong, *Investigation on control strategies of pneumatic nonlinear systems and their applications*, Doctoral Dissertation, Xi'an Jiaotong University, Xi'an, 2003 (in Chinese).

[5] J. S. Jang, Y. B. Kim and I. Y. Lee *et al*, "Design of a synchronous position controller with a pneumatic cylinder driving system", in *Proc. of the 2004 SICE Annual Conference*, Sapporo, Japan, 2004, 295-299.

[6] S. Shibata, T. Yamamoto and M. Jindai, A synchronous mutual position control for vertical pneumatic servo system, *JSME International Journal, Series C: Mechanical Systems, Machine Elements and Manufacturing*, vol.49, no.1, 2006, pp 197-204.

[7] M. Smaoui, X. Brun and D. Thomasset, A study on tracking position control of an electropneumatic system using backstepping design, *Control Engineering Practice*, vol.14, no.8, 2006 pp 923-933.

[8] S. R. Pandian, F. Takemura and Y. Hayakawa *et al*, Pressure observer-controller design for pneumatic cylinder actuators, *IEEE/ASME Transactions on Mechatronics*, vol.7, no.4, 2002, pp 490-499.

[9] S. Shibata, M. Jindai and T. Yamamoto *et al*, A disturbance estimation type control for pneumatic servo system using neural network, *JSME International Journal, Series C: Mechanical Systems, Machine Elements and Manufacturing*, vol.49, no.1, 2006, pp 189-196.

[10] X. Shen, J. Zhang and E. J. Barth *et al*, Nonlinear model-based control of pulse width modulated pneumatic servo systems, *Transaction of the ASME. Journal of Dynamic Systems, Measurement and Control*, vol.128, no.3, 2006, pp 663-669.

[11] Xiaocong Zhu, Guoliang Tao, Bin Yao and Jian Cao, Adaptive robust posture control of a parallel manipulator driven by pneumatic muscles, *Automatica*, vol.44, no.9, 2008, pp 2248-2257.

[12] Jian Cao, Xiaocong Zhu, Guoliang Tao and Bin Yao, Adaptive robust tracking control of pressure trajectory based on Kalman filter, *Chinese Journal of Mechanical Engineering*, (Submitted).

[13] E. Richer and Y. Hurmuzlu, A high performance pneumatic force actuator system: Part I-nonlinear mathematical model, *Transactions of the ASME. Journal of dynamic systems, measurement, and control*, vol.122, no.3, 2000, pp 416-425.

[14] Z. MOZER, A. TAJTI and V. SZENTE, "Experimental investigation on pneumatic components", in *Proc. of the 12th International Conference on Fluid Flow Technologies*, Budapest, Hungary, 2003, pp. 517-524.

[15] B. Yao and M. Tomizuka, Adaptive robust control of MIMO nonlinear systems in semi-strict feedback forms, *Automatica*, vol.37, no.9, 2001, pp 1305-1321.

[16] B. Yao, "Integrated direct/indirect adaptive robust control of SISO nonlinear systems in semi-strict feedback form", in *Proc. of the American Control Conference*, Denver, USA, 2003, pp. 3020-3025.